

Properties of rotating two-component Bose-Einstein Condensates

I. Corro¹, R.G. Scott² and A.M. Martin¹¹ School of Physics, University of Melbourne, Parkville, Victoria 3010, Australia.² School of Physics and Astronomy, University of Nottingham, Nottingham NG7 2RD, U.K.

We derive equations of motion for rotating two-component Bose-Einstein Condensates, finding multiple solutions. Stability analysis of these solutions and comparison with Truncated Wigner simulations enables us to identify the regimes for which giant multiply quantized vortices and interlocking vortex lattices will occur. In addition, our analysis predicts novel center of mass oscillations.

PACS numbers: 03.75.Kk, 03.75.Mn, 03.75.Lm

A two-component Bose-Einstein Condensate (TCBEC) exhibits a wide range of interesting behaviour that has been the subject of much theoretical and experimental research. The two components may form either overlapping, or separated phases exhibiting complex topological properties [1, 2, 3, 4]. For the case of a rotating TCBEC the different ground state structures are even more numerous. Interlocking triangular and square vortex lattices have been predicted theoretically [5], and confirmed experimentally [6]. Recently, a number of papers have also predicted, through thermodynamic arguments, the possibility of forming multiply quantized vortices [7, 8]. Such an object is unstable for a single component BEC in a harmonic trap [9] and its realisation would be a striking consequence of the interpenetration of superfluid components.

In this letter we investigate the dynamics of a rotating TCBEC. As in the one component case [10], instabilities in quadrupolar oscillations lead to turbulence, which in turn allows for the creation of non trivial geometries. As such, we analytically determine the conditions under which a rotating TCBEC is stable/unstable. Investigating the system using Truncated Wigner simulations, generalised to the two-component case to account for quantum fluctuations, shows that these instabilities lead to the formation of the interlaced vortex lattices and giant multiply quantized vortices described above. We are therefore able to give explicit criteria for the creation of these exotic structures. Our analytical results also predict novel centre of mass instabilities, which result in interesting behaviour such as both components separating and orbiting around each other.

For single component BECs, considerable theoretical [10, 11, 12, 13, 14, 15] and experimental [16, 17, 18] effort has been applied to understanding their properties under rotation. An interesting result of this investigation has been that thermodynamics does not correctly predict the emergence of vortices. Instead, the dynamic motion of a rotating BEC must be investigated. In practice, a BEC can be stirred by introducing a rotating anisotropy into the confining potential. If done adiabatically, the BEC will gradually deform and begin to rotate with the anisotropy. The equations of motion can

then be found by considering static solutions in the rotating frame. Here, we extend this analysis to the two component case.

A TCBEC can be described by 2 mean-field wavefunctions (ψ_1 and ψ_2) whose time evolution is dictated by the coupled two-component Gross-Pitaevskii Equation (GPE) [19]. To do this, the GPE in the frame rotating with the potential is transformed using $\psi_j = \sqrt{n_j} e^{i\phi_j}$ (n_j is the density of component j , rescaled by a constant n_0 , and ϕ_j is the phase), and the Thomas-Fermi Approximation (TFA) [20] is applied, giving the hydrodynamic equations of motion:

$$\frac{\partial \psi_j}{\partial t} = -i \mu_j (\psi_j - \psi_j^*) \quad (1)$$

$$\frac{\partial \phi_j}{\partial t} = \mu_j + g_{jj} n_j + g_{12} n_{j^0} \quad (2)$$

$$\mu_j = \frac{m_j}{2} \dot{\phi}_j^2 + V_j - m_j r_j \dot{\phi}_j \quad (3)$$

where the j subscripts ($j = 1$ or 2) refer to the component under consideration and $j^0 \notin j$. m_j is the mass and $\mu_j = \mu_j(\mathbf{y}; \mathbf{x}; 0)$ is the angular rotation frequency of both species' traps, about the z -axis. Since we are concerned with stationary solutions, only the case $\dot{\phi}_1 = \dot{\phi}_2$ is considered, as otherwise time can not be removed from the Hamiltonian. The trapping is that of a harmonic elliptic trap $V_j = \frac{m_j}{2} [(1 - \epsilon_j)^2 x^2 + (1 + \epsilon_j)^2 y^2 + \epsilon_j^2 z^2]$. ϵ_j , ϵ_{zj} and μ_j are respectively the ellipticity in the x - y plane, the frequency in the z direction, and the frequency in the x - y plane when $\epsilon_j = 0$. The intra (inter) species interaction coefficients are $g_j = 4n_0 \epsilon_j^2 a_j = m_j (g_{12} = 2n_0 \epsilon_j^2 a_{12} [m_1 + m_2] = [m_1 m_2])$, where a_j and a_{12} are the intra and inter species scattering lengths respectively. We will consider only g_1 and g_2 positive as the TFA is not valid for attractive interactions.

Steady state solutions in the rotating frame are obtained by setting $\frac{\partial \psi_j}{\partial t} = 0$ and $\frac{\partial \phi_j}{\partial t} = \mu_j$ the chemical potential of species j . Solving Eq. (2) gives two possible solutions for the density. If the density of both components is non zero then

$$\frac{\mu_j}{g_j} = \frac{g_{j^0} (n_j - n_{j^0}) - g_{12} (n_{j^0} - n_j)}{g_j g_{j^0} - g_{12}} \quad (4)$$

If one of the components has zero density, then the solution for the other component is

$$j^{(o)} = \frac{1}{g_j} (j^{(c)} - j^{(o)}): \quad (5)$$

Regions in the BEC where Eq. (4) is applicable will be referred to as the central region (indicated by superscript c) as this usually occurs in the middle of the BEC. Regions where Eq. (5) is applicable will be referred to as the outer region (indicated by superscript o). As in the one-component case, the TFA has the effect that j can become negative [20]. When this is the case, we assume that $j = 0$. Given the above, the total density for each component can be expressed as

$$j = j^{(c)} H(\frac{r}{r_1}) H(\frac{r}{r_2}) + j^{(o)} H(\frac{r}{r_1}) H(\frac{r}{r_2}); \quad (6)$$

where $H(x) = 0$ for $x < 0$ and $H(x) = 1$ for $x > 0$. Without rotation ($\omega = r_1 = r_2 = 0$), Eq. (6) corresponds to that derived in Refs. [1, 2].

Numerically solving the GPE shows that a TCBECD displays the following behaviour: $\frac{g_1}{g_2} < g_{12} < \frac{g_2}{g_1}$ is the overlapping phase. When $\frac{g_2}{g_1} < g_{12} < \frac{g_1}{g_2}$, 1 begins to dip in the middle. $g_{12} > \frac{g_1}{g_2}$ is the separated phase where component 1 forms a shell around component 2 [21]. It has been shown [3] that the accuracy of the TFA depends on the parameters used. We have conducted extensive comparisons between the TFA and full GPE solutions, identifying the following conditions for TFA validity: For $\frac{g_1}{g_2} < g_{12} < \frac{g_2}{g_1}$ we find excellent agreement, with accuracy consistent with the results presented in Ref. [3] ($g_{12} = \frac{g_2}{g_1}$ is the point where the TFA predicts j_1 reaches 0 at $r = 0$). As the point $g_{12} = \frac{g_2}{g_1}$ is approached the TFA results deviate from the full GPE results, but remain qualitatively correct for $\frac{g_2}{g_1} < g_{12} < \frac{g_1}{g_2}$. For $g_{12} < \frac{g_1}{g_2}$ and $g_{12} > \frac{g_1}{g_2}$ the results are completely incorrect. In what follows we therefore consider the TFA solutions only in the region of their validity: $\frac{g_1}{g_2} < g_{12} < \frac{g_2}{g_1}$.

For the rotating case, Eq. (6) is still valid, and the phase is found by inserting a quadrupolar oscillation ansatz $j = [j^{(c)} H(\frac{r}{r_1}) H(\frac{r}{r_2}) + j^{(o)} H(\frac{r}{r_1}) H(\frac{r}{r_2})] \chi y$ and Eq. (6) into Eq. (1) and solving for the j 's. The j 's are real constants representing the magnitude of the quadrupolar oscillation. For $j^{(o)}$ this gives:

$$j^{(o)3} - 2j^{(o)2} + j^{(o)} = 0; \quad (7)$$

which has up to 3 real solutions and is identical to the one component case [10]. For the $j^{(c)}$'s we get two simultaneous equations:

$$2g_{12}m_j - j^{(c)2} + j^{(c)} + j^{(c)}j^{(o)} = 0; \quad (8)$$

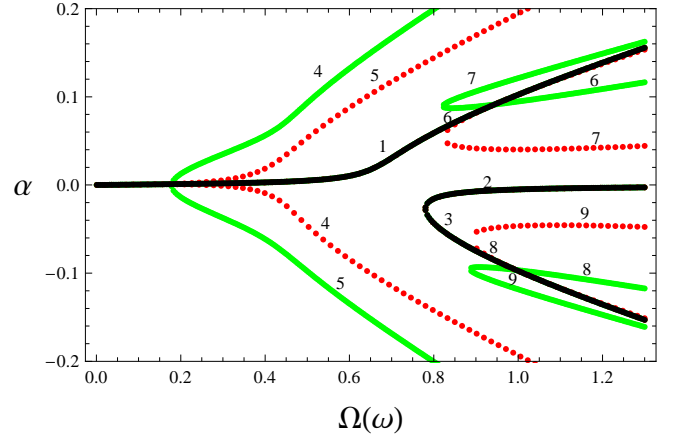


FIG. 1: The 9 solutions of the $j^{(c)}$'s given the parameters for a Rb-Cs system (see text) with $g_{12} = 0.4$; $g_1 = g_2 = 0.05$. $j_1^{(c)}$ shown in (green), $j_2^{(c)}$ (red dots), $j^{(o)}$'s (black). $j_1^{(o)} = j_2^{(o)}$ (see text) and the three $j^{(o)}$ branches are equal to three of the nine $j^{(c)}$ branches. The numbering allows matching of each $j_1^{(c)}$ solutions to the corresponding $j_2^{(c)}$ solution.

This yields up to nine real solutions for $f_1^{(c)}$; $f_2^{(c)}$ g , three of which are the same as the three solutions to $f_1^{(o)}$; $f_2^{(o)}$ g . Therefore in the outer region, the solutions for f_1 and f_2 are exactly the same as in the one component case. In the central region the solutions are more numerous and display a complicated dependence on the parameters in the system.

For simplicity we therefore focus on parameter values that describe ^{87}Rb - ^{133}Cs mixtures. This case is particularly simple as $m_{\text{Rb}} = m_{\text{Cs}}$. Also, the scattering length of Cs can be tuned via a Feshbach resonance [22]; here we choose $a_1 = a_2$. $m_{\text{Cs}} > m_{\text{Rb}}$ making Cs component 2 by definition. Results will be given in dimensionless units: $n_0 = 4 \cdot 10^{18} \text{ m}^{-3}$, $\text{Length} = 1.919 \cdot 10^6 \text{ m}$, $\text{Time} = 5.047 \cdot 10^3 \text{ s}$, $\text{Mass} = 1.447 \cdot 10^{25} \text{ Kg}$. The interspecies scattering length is unknown for this system, therefore results for varying g_{12} are given throughout. With these units the parameters become $g_1 = g_2 = 1$, $g_{12} = 0.654$, $m_2 = 1.529$, $\frac{g_2}{g_1} = 0.808$, $\frac{g_2}{m_2} = 0.428$, and we choose $\omega = 0.1$.

An example of the 9 solutions to Eq. (8) for $f_1^{(c)}$; $f_2^{(c)}$ g is shown in Fig. 1. Each branch represents a different static solution for a rotating TCBECD, each with quadrupolar oscillations of different magnitudes. Branches 1-3 are equal to the 3 solutions for $f_1^{(o)}$; $f_2^{(o)}$ g and because $m_1 = m_2$, $j_1^{(o)} = j_2^{(o)}$. When $j_1^{(c)} \neq j_2^{(c)}$ (branches 4-9), the density of the central and outer regions do not join continuously. Therefore, these TFA solutions do not correctly describe the interface between the two regions and can not be used in the stability analysis that follows. Branches 1 and 2 have the lowest energy and are also the easiest to access. Branch 3 is always unstable. As in the one component case, branch 1 is accessed by ramping keeping fixed or by ramping and

keeping $\langle p \rangle < \frac{p}{2}$ fixed. Branch 2 is accessed by ramping with $\langle p \rangle > \frac{p}{2}$ fixed [1].

Stability can be analysed by linearising Eqs. (1,2) about the critical points. The simple quadratic form of these solutions, Eqs. (4,5), allows for analytical solutions. However, this requires that both the central and outer region of the density profile be considered independently. For $g_{12} < 0$, the two components are pulled together tightly and the central region dominates the density profile of the BEC, and therefore also controls BEC stability. For $g_{12} > 0$, component 1 is forced outwards and component 2 inwards as the separated phase is approached. As g_{12} increases, the density in the central region of component 1 goes from having a maximum, to having a minimum at $r = 0$. The stability of this central region is then dependent on its connection with the outer region and can not be considered independently. Therefore, as an approximation, for $g_{12} > 0$ we use the outer region to calculate the stability of component 1 and use the central region to calculate the stability of component 2, thereby neglecting interactions of collective modes from different species [24].

With the above discussion in mind, we consider infinitesimal perturbations $\psi_j = \psi_j + \delta\psi_j$ and $\psi_j = \psi_j + \delta\psi_j$, with $\psi_j = \psi_j + \delta\psi_j$ being a set of static solutions to Eqs. (1,2). This gives the following equations of motion for the collective modes:

$$\frac{\partial}{\partial t} \begin{pmatrix} \psi_1 \\ \psi_2 \end{pmatrix} = \begin{pmatrix} A_1 & 0 \\ 0 & A_2 \end{pmatrix} \begin{pmatrix} \psi_1 \\ \psi_2 \end{pmatrix} \quad (9)$$

$$A_j = \begin{pmatrix} v_{rj} & r \\ r & (v_{rj} - \frac{g_j}{m_j}) \end{pmatrix} v_{rj} \quad ; \quad (10)$$

where $v_{rj} = \frac{1}{m_j} r \cdot \nabla \psi_j$ is the wave function velocity in the rotating frame at position r . For $g_{12} < 0$, ψ_1 and ψ_2 are both given by Eq. (4), and $B = 1$. For $g_{12} > 0$, ψ_1 is given by Eq. (5) and ψ_2 by Eq. (4) with $B = 0$.

As in the one component case [10], we find that the eigenfunctions of Eq. (9) are polynomials of the form $\psi_j = \sum_{pqr} c_{pqr} x^p y^q z^r$, $\psi_j = \sum_{pqr} c_{pqr} x^p y^q z^r$, where c_{pqr} and c_{pqr} are constants. The BEC is unstable when one of the eigenvalues has a positive real part. We find that a TC BEC is always unstable for parameters with which a one component BEC is, and is also unstable elsewhere. Hence, under rotation, the presence of a second component destabilises a BEC.

As an example we again choose the case of Rb and Cs. Fig. 2 shows regions of instability for ω and Ω for four different values of g_{12} [25]. Black indicates regions where both a one-component and TC BEC are unstable and red indicates regions where only a two-component BEC is unstable.

To complement these Thomas-Fermi results we have adapted 2D Truncated Wigner simulations [23] to the

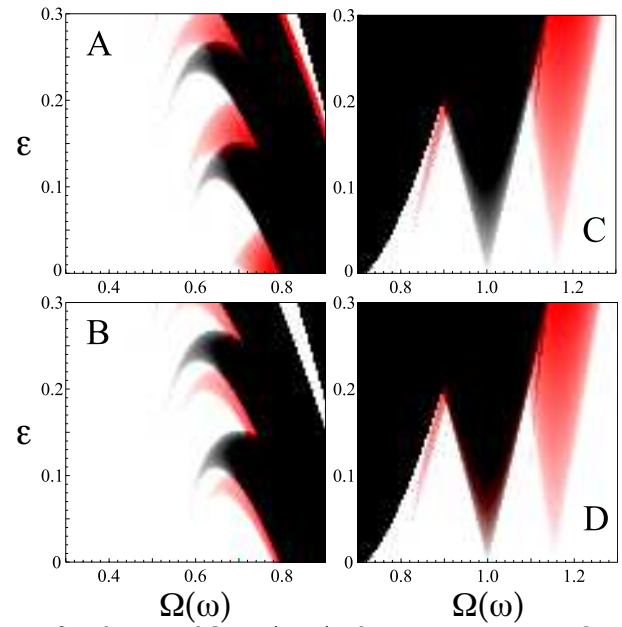


FIG. 2: The unstable regions in the parameter space for the Rb-Cs mixture with $\mu_1 = \mu_2 = \mu$. $g_{12} = 0.3$ (A), 0.5 (B), 0.6 (C), -0.1 (D). (A) and (B) are branch 1, (C) and (D) are branch 2. Black: regions where both a one-component and a TC BEC are unstable. Red: regions where only a TC BEC is unstable. (C) and (D) show the two intra-species COM instabilities centred at $\mu_1 = \mu_2 = \mu$, with the classical COM instability centred at $\mu = \mu$.

two-component case, and investigated the instabilities predicted in Fig. 2. As in the one component case [14, 15], the TFA description of the instabilities gives good quantitative agreement with simulations. The results of typical simulations are given in Fig. 3. In the overlapping phase, the simulations show that when an instability is reached, the BEC becomes turbulent and vortices enter. They then form an interlaced vortex lattice [Fig. 3 (A, B)]. This state is of the same type as has been seen to form in experiments when a one-component BEC with a vortex lattice already present was split into two hypernetic components [6]. The simulations show strong density peaks in each component at the locations of the other component's vortex cores.

Although not within the regime of TFA validity, we can expect that in the separated phase, the TC BEC will be unstable at least where a one component BEC is. Using this, we investigated the behaviour of the rotational instabilities in the separated phase. In this phase the outer component has almost zero density in the centre. When instability is reached, simulations show that multiple vortices push their way through the outer shell into the low density centre of component 1. These vortices congregate, forming a giant vortex of multiple quantization Fig. 3 (C, D). Normally, two overlapping vortices are predicted to be thermodynamically unstable [9]. However, in this system the large density of the Cs component attracts them to the centre while the outer shell of Rb holds them in. In general, these vortex states do not

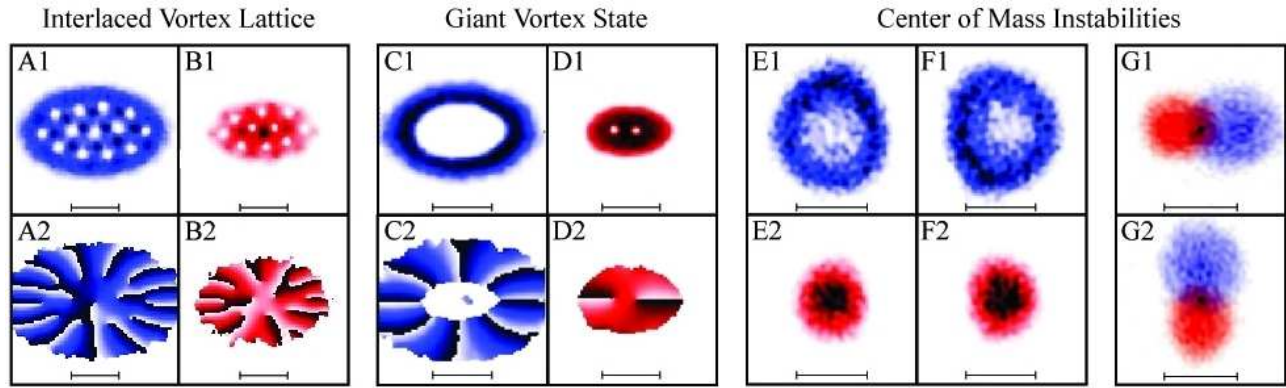


FIG. 3: Results of 2D Truncated Wigner simulations with Rb (blue) and Cs (red) having equal norms of $3:761 \times 10^9 \text{ m}^{-1}$. The horizontal bar denotes $40 \text{ } \mu\text{m}$. (A1,C1) is the density and (A2,C2) the phase of component 1. (B1,D1) is the density and (B2,D2) the phase of component 2. (E,F) is the intra-species COM instability $g_{12} > 0$ case: (F) is the density shortly after (E) showing component 2 (E2,F2) bouncing off the shell of the enclosing component 1 (E1,F1). (G) is the intra-species COM instability for $g_{12} < 0$. (G2) is the density shortly after (G1) showing the two components rotating around each other.

share angular momentum equally between species. This multiply quantized vortex has recently been predicted thermodynamically [7, 8]. These results show how in practice such a state could be created, and crucially give the criterion for its existence: $g_{12} > \sqrt{g_1 g_2}$.

Branch 2 also shows interesting behaviour. For a one component BEC, the main feature is the centre of mass (COM) instability [Fig. 2C, 2D], which is the same as that experienced by a classical particle in a rotating elliptical potential [11]. For the one component case, this causes the BEC to be ejected from the trap [14] and it is present when $|\Omega| < \Omega_c$ [26]. However, in the two component case, we find that as g_2 is increased, the COM instability splits into 2 parts with the two-component instability [Fig. 2C - red] shifting away from the classical COM instability, which is unaffected by g_{12} . Simulations confirm these predictions, showing that when this instability is reached, the COM of the combined BEC is unaffected, but the COM of each individual component becomes unstable. When component 2 reaches this intra-species COM instability, it begins to move away from the trap centre. However, it is trapped; it begins bouncing off the surrounding shell formed by the Rb [Fig. 3 (E,F)]. No vortices form during this instability.

Finally, for $g_{12} < 0$ the COM instability again splits into 2 parts [Fig. 2D - red]. In this case the two components overlap and neither is bound within the other. When the intra-species COM instability is reached this time, they begin to separate and exit the trap, but the instability is caused purely by their interaction and the effect diminishes as they separate. This results in the two components partially separating and orbiting around each other [Fig. 3 (G)]. Again, no vortices form.

These results illustrate that mixtures produce a rich variety of dynamical regimes, which may be accessed by tuning experimental parameters. We have examined the applicability of the TFA to a TC BEC and extended it

to the rotating case allowing us to find conditions under which interlaced vortex lattices and giant multiply quantized vortices will spontaneously form. In addition, we find novel centres of mass instabilities. These occur in the $|\Omega| > \Omega_c$ regime, and can be observed through pronounced macroscopic oscillations of the individual BEC components.

We thank Simon Cornish for helpful discussions and acknowledge funding from the ARC (IC and AMM) and the EPSRC (RGS).

-
- [1] T.-L. Ho and V. B. Shenoy, Phys. Rev. Lett. 77, 3276 (1996).
 - [2] F. Riboli and M. Modugno, Phys. Rev. A 65, 063614 (2002).
 - [3] H. Pu and N. P. Bigelow, Phys. Rev. Lett. 80, 1130 (1998).
 - [4] B. D. Esry et al, Phys. Rev. Lett. 78, 3594 (1997).
 - [5] E. J. Mueller and T.-L. Ho, Phys. Rev. Lett. 88, 180403 (2002).
 - [6] V. Schweikhard et al, Phys. Rev. Lett. 93, 210403 (2004).
 - [7] J. Christensson et al, N. J. Phys. 10, 033029 (2008).
 - [8] S.-J. Yang et al, preprint, arXiv:0712.2945 (2007).
 - [9] Y. Castin and R. Dum, Eur. Phys. J. D 7, 399 (1999).
 - [10] S. Sinha and Y. Castin, Phys. Rev. Lett. 87, 190402 (2001).
 - [11] A. Recati, F. Zambelli, and S. Stringari, Phys. Rev. Lett. 86, 377 (2001).
 - [12] M. Tsubota, K. Kasamatsu, and M. Ueda, Phys. Rev. A 65, 023603 (2002).
 - [13] E. Lundh, J.-P. Martikainen, and K.-A. Suominen, Phys. Rev. A 67, 063604 (2003).
 - [14] I. Corro, N. G. Parker, and A. M. Martin, J. Phys. B 40, 3615 (2007).
 - [15] N. G. Parker, R. M. van Bijnen, and A. M. Martin, Phys. Rev. A 73, 061603 (2006).
 - [16] K. W. Madison et al, Phys. Rev. Lett. 84, 806 (2000).

- [17] K. W. Madison, F. Chevy, V. Bretin, and J. Dalibard, Phys. Rev. Lett. 86, 4443 (2001).
- [18] E. Hodby et al., Phys. Rev. Lett. 88, 010405 (2001).
- [19] C. J. Pethick, Bose-Einstein Condensation in Dilute Gases (Oxford University Press, Cambridge, 2003).
- [20] G. Baym and C. J. Pethick, Phys. Rev. Lett. 76, 6 (1996).
- [21] E. Timmermans, Phys. Rev. Lett. 81, 5718 (1998).
- [22] S. Inouye et al., Nature 392, 151 (1998).
- [23] M. J. Steel et al., Phys. Rev. A 58, 4824 (1998).
- [24] This is valid for g_{12} small, and also for $g_{12} > g_2 \frac{m_1}{m_2}$ because repulsive interactions mean that there is little inter-species overlap and so inter-species interactions are negligible. Note that g_{12} is still significant through Eq. (4)
- [25] We have used polynomials of order 7, larger orders produce no significant contribution.
- [26] The confining potential and BEC, rather than rotating, can be thought of as oscillating in such a way as to be invariant in a rotating frame. Therefore, thermodynamic arguments restricting a stable confined rotating gas to the region $\Omega < \Omega_c$ do not apply.